Computing Geodesic Spectra of Surfaces

Miao Jin [*] Stony Brook University
Feng Luo[†] Rutgers University
Shing-Tung Yau[‡] Harvard University
Xianfeng Gu[§] Stony Brook University

Abstract

Surface classification is one of the most fundamental problems in geometric modeling. Surfaces can be classified according to their conformal structures. In general, each topological equivalent class has infinite conformally equivalent classes.

This paper introduces a novel method to classify surfaces by their conformal structures. Surfaces in the same conformal class share the same uniformization metric, which induces constant Gaussian curvature everywhere on the surface. Under the uniformization metric, each homotopy class of a closed curves on the surface has a unique geodesic. The lengths of all closed geodesics form the geodesic spectrum. The map from the fundamental group to the geodesic spectrum completely determines the conformal structure of the surface.

We first compute the uniformization metric using discrete Ricci flow method, then compute the Fuchsian group generators, finally deduce the geodesic spectra from the generators in a closed form.

The method is rigorous and practical. Geodesic spectra is applied as the signature of surfaces for shape comparison and classification.

CR Categories: I.3.5 [Computer Graphics]: Computational Geometry and Object Modeling—Geometric algorithms;

Keywords: Geodesic Spectrum, Surface Classification, Ricci Flow, Uniformization, Conformal Structure,

1 INTRODUCTION

Surface matching and classification are fundamental problems in geometric modeling, computer graphics and computer vision. Surfaces can be classified according to their geometric structures, such as topological structure, conformal structure or the Riemannian metric structure.

Comparing to topological classification, conformal classification is much refiner. Each topological equivalent class has infinite conformally equivalent classes. Comparing to classification by metrics, conformal classification is efficient to compute and robust to noises. Further more, the dimension of conformal classes within the same topological class is finite, therefore the conformal class can be indicated by a small set of numbers, whereas the dimension of metric classes for the same topology is infinite.

In this work, we propose to use geodesic spectra as the "fingerprint" of the conformal structure of a general surface. It has many real applications, such as surface classification, surface comparison, shape retrieval etc.

The computational process involves some advanced topological and geometric concepts. We briefly explain the main ideas and the intuitions in the following discussion. Their rigorous definitions and more references will be given in section 3. We illustrate the major concepts by real examples: Genus one surface case shown in Figures 2, 3, and 6; High genus surface case demonstrated in Figures 4, 5 and 6.

1.1 Main Ideas

Our ultimate goal is to classify surfaces by their conformal structures. Two surfaces are conformally equivalent, if there exists a homeomorphism between them, which is angle preserving. It is extremely challenging to find such an angle preserving map directly. Instead, we convert the conformal classification problem to computing geodesic spectrum. The following discussion will briefly explain the intuition of this idea.

Converting Conformal Map to. Isometry
Suppose two surfaces Σ_1, Σ_2 with the Euclidean metrics $\mathbf{g}_1, \mathbf{g}_2$ are embedded in $\mathbb{R}^3$ with the same topology. A map between them $f : \Sigma_1 \to \Sigma_2$ is conformal, if it preserves angles.

According to Riemann uniformization theorem, given a metric surface $(\Sigma, \mathbf{g})$, there exists functions $u : \Sigma \to \mathbb{R}$, such that the new metric $\bar{\mathbf{g}} = e^{2u}\mathbf{g}$ induces constant Gaussian curvature on Σ. The constant is $+1, 0, -1$, if Euler number of Σ is positive, zero and negative respectively. Such a metric is called the uniformization metric of Σ, and e^{2u} is called the conformal factor. Under the uniformization metrics, the conformal map $f : (\Sigma_1, \bar{\mathbf{g}}_1) \to (\Sigma_2, \bar{\mathbf{g}}_2)$ is an isometry.

Converting Isometry Verification to Geodesic Spectra Comparison
In order to test whether a map is an isometry, we consider the geodesics on the surfaces. A geodesic is a locally shortest curve, which is solely determined by the metric, and reflects the intrinsic properties of the metric.

Suppose $f : (\Sigma_1, \bar{\mathbf{g}}_1) \to (\Sigma_2, \bar{\mathbf{g}}_2)$ is an isometry, γ_1 is a closed geodesic on Σ_1 under the metric $\bar{\mathbf{g}}_1$, then $f(\gamma_1)$ is also a closed geodesic on Σ_2 under $\bar{\mathbf{g}}_2$. Further more the lengths of γ_1 and $f(\gamma_1)$ are the same. We can sort all the closed geodesics on Σ_1 according to their lengths in ascending order $\{\gamma_1, \gamma_2, \gamma_3, \cdots\}$, then $\{f(\gamma_1), f(\gamma_2), f(\gamma_3), \cdots\}$ are the corresponding ordered geodesics on Σ_2. The lengths of the above geodesic sequence form the geodesic spectrum. Therefore, if two surfaces are isometric, they share the same geodesic spectrum, which can be computed individually without any knowledge of the map.

[*] e-mail: mjin@cs.sunysb.edu
[†] e-mail:fluo@math.rutgers.edu
[‡] e-mail:yau@math.harvard.edu
[§] e-mail:gu@cs.sunysb.edu

Converting Geodesic length to Matrix Eigenvalue
Suppose Σ of negative Euler number has uniformization metric $\bar{\mathbf{g}}$, which induces -1 Gaussian curvature everywhere. Then locally, Σ can be isometrically embedded in the hyperbolic space $\mathbb{H}^2$. The local embedding can be extended/developed, such that the whole surface is periodically embedded in $\mathbb{H}^2$. A closed geodesic on the surface is developed to a hyperbolic line segment on $\mathbb{H}^2$. A unique hyperbolic rigid motion can be directly computed which maps the hyperbolic line to itself and the starting point of the segment to its end point. The eigenvalue of the matrix representation of this rigid motion is exactly the length of the closed geodesic.

All homotopy classes on the surface can be traversed using symbolic computation and represented as a string; Each homotopy class has a unique closed geodesic, whose corresponding rigid motion can be computed directly from the string and represented as a matrix; The geodesic length can be derived from the eigenvalues of the matrix. Therefore, the geodesic spectrum can be efficiently and accurately computed.

The remainder of the paper is organized as follows. Section 2 contains a summary of most related works. Section 3 briefly introduces the necessary theoretic background to design the algorithm. Section 4 describes our algorithms in details. Section 5 presents results of our experiments on general models. We summarize the paper and point out future directions in the final section 6.

2 Related Works

Geodesics. Computing geodesic paths on discrete setting has been intensively studied in the literature. The MMP algorithm [Mitchell et al. 1987] firstly provided an exact solution for the single source, all destination shortest path problem on a triangle mesh. [Surazhsky et al. 2005] implemented this algorithm, and extend with a merging operation to obtain computationally efficient (running time $O(n\log n)$) and accurate approximations with bounded error. Other works include an exact geodesic algorithm with worst case time complexity of O(n2) described by [Chen and Han 1996] and partially implemented by [KANEVA and OROURKE 2000], an algorithm for the single source, single destination geodesic path between two given mesh vertices, in $O(nlog2n)$ time described by [Kapoor 1999], and a variation of the fast-marching method to compute approximate geodesics on meshes in $O(nlogn)$ time by [KIMMEL and SETHIAN 1998]. [Dey 1994] proposes an improved algorithm for detecting null-homotopic cycles on compact 2-manifolds without boundary. An approach to compute closed geodesics on surfaces constriction computation using surface curvature is introduced in [Hetroy 2005]. An algorithm with polynomial running time to compute a shortest simple loop homotopic to a given simple loop is in [Éric Colin de Verdiére and Lazarus 2002]. Our method to compute geodesics are purely algebraic, simple and no local minimal problem.

Surfaces Classification There are a lot of research works on surfaces classification. The most related one for surface classification by conformal structure has been introduced in [Gu and Yau 2003b] using period matrices. Their method cannot avoid the intrinsic ambiguity of the homotopy. Current geodesic spectrum approach does not have the ambiguity and is better suited for the practical applications. [Elad and Kimmel 2003] proposes a surface classification method that uses bending invariant signatures based on geodesic circles around some key points on the surface, but the selection of corresponding key points may also introduce ambiguity. A Multiresolutional Reeb Graph constructed based on computation of Euclidean geodesic distance is used to measuring similarity in [Hilaga et al. 2001]. [Reuter et al. 2005] extracts fingerprints of surface by taking the eigenvalues of its respective Laplace-Beltrami operator. And Other more statistical approaches include [Osada et al. 2001].

Ricci Flow. Ricci flow we used in this paper to compute surface uniformization metric was first introduced by Hamilton [Hamilton 1988], and later it is generalized to discrete cased [Chow and Luo 2003]. It has been applied for constructions of manifold splines [Gu et al. 2005] and geometric structures on general surfaces [Jin et al. 2006].

Circle Packing and Circle Pattern. Circle packing was first introduced by Thurston in [Thurston 1976], where he designed an algorithm to find the circle packing of a graph by adjusting the radii at vertices one at a time. Stephenson et al. improved the algorithm and developed practical algorithms in [Stephenson 2005]. Circle pattern is introduced in [Bobenko and Schroder 2005] and [Kharevych et al. 2005], which is closely related to circle packing. Instead of using circles centered at each vertex, this method uses the circum-circles of triangles.Both circle packing and circle pattern can be applied for approximating conformal deformation.

3 THEORETICAL BACKGROUND

In this section, we briefly introduce several important concepts in topology and Riemann Geometry, also a brief review of discrete Ricci flow, which we need in our algorithms. For more details, we refer readers to [Thurston 1997] and [Chow and Luo 2003]. Due to page limit, we refer readers to [Mika Seppala 1992] for every equations and models we used in this paper for hyperbolic geometry.

3.1 Uniformization Theorem

Theorem 1 (Uniformization Theorem) *Let $(\Sigma,\mathbf{g})$ be a compact 2-dimensional Riemannian manifold, then there is a metric $\bar{\mathbf{g}}$ conformal to $\mathbf{g}$ which has constant Gauss curvature.*

Such a metric is called the *uniformization metric*. All closed surfaces can be conformally mapped to three canonical spaces, the sphere for genus zero surfaces with $\chi > 0$, the plane for genus one surfaces with $\chi = 0$, and the hyperbolic space for high genus surfaces with $\chi < 0$.

There are two common models for the hyperbolic space $\mathbb{H}$: Poincaré disk model and upper half plane model. The conversion from the upper half plane model to the Poincaré disk model is given by

$$h = \frac{iz+1}{z+i}. \tag{1}$$

In our work, we use both models.

3.2 Geodesic Spectrum

The geodesics are the locally shortest curves on surfaces, closely related to metric. The geodesic lengths reflects the global information of the surface. On general surfaces, there may be multiple geodesics in each homotopy class. For surfaces with uniformization metrics, the geodesics are unique in each homotopy class.

Theorem 2 (Geodesic Uniqueness) *Suppose* $(\Sigma, \mathbf{g})$ *is a closed compact surface with Riemannian metric* $\mathbf{g}$*, if Gauss curvature is negative everywhere, then each homotopy class has a unique geodesic.*

The proof is based on Gauss-Bonnet theorem. We refer readers to [Mika Seppala 1992] for details.

For our study of conformal structures, we can always deform the surface metric to the uniformization metric, then the geodesic lengths in each homotopy class form the length spectrum.

Definition 3 (Length Spectrum) *Let* $(\Sigma, \bar{\mathbf{g}})$ *be a surface with uniformization metric, the set of the lengths of closed geodesics on* Σ *is called the length spectrum of the surface* Σ*.*

The number of homotopy class of closed curves on a compact surface is countable. Since each homotopy class contains only one geodesic curve, also the length spectrum of a Riemann surface is countable. If two surfaces are conformally equivalent, they have same length spectra.

3.3 Discrete Surface Ricci Flow

The Riemannian metric on an Euclidean or hyperbolic mesh S (we say a mesh is Euclidean or hyperbolic if all its faces are Euclidean or hyperbolic.) is determined by its edge lengths. Therefore we define the discrete Riemannian metric on a mesh as its edge lengths, $l : E \to \mathbb{R}^+$, such that for a face $\{i, j, k\}$, the edge lengths satisfy the triangle inequality, $l_{ij} + l_{jk} > l_{ki}$..

A *weight* on the mesh is a function $\Phi : E \to [0, \frac{\pi}{2}]$, on each edge e_{ij}. A *radius* on the mesh is a function $\Gamma : V \to \mathbb{R}^+$, on each vertex v_i by assigning a positive number γ_i. They realize each edge e_{ij} joining v_i to v_j by a Euclidean segment of length

$$l_{ij} = \sqrt{\gamma_i^2 + \gamma_j^2 + 2\gamma_i\gamma_j \cos\Phi(e_{ij})}. \quad (2)$$

And for each face $\{l_{ij}, l_{jk}, l_{ki}\}$ satisfy triangle inequality. In hyperbolic case, the length can be deduced from hyperbolic cosine law

$$l_{ij} = \cosh^{-1}(\cosh\gamma_i \cosh\gamma_j + \sinh\gamma_i \sinh\gamma_j \cos\Phi(e_{ij})). \quad (3)$$

Definition 4 (Circle Packing Metric) *The pair of vertex radius function and edge weight function on a mesh* Σ $\{\Gamma, \Phi\}$ *is called a circle packing metric of* Σ*.*

Definition 5 (Conformal Circle Packing Metrics) *Two circle packing metrics* $\{\Gamma_1, \Phi_1\}$ *and* $\{\Gamma_2, \Phi_2\}$ *are conformally equivalent, if* $\Phi_1 \equiv \Phi_2$*.*

Therefore, a conformal deformation of a circle packing metric only modifies the vertex radii.

Discrete Gauss Curvature The discrete Gauss curvature is defined as the angle deficit on a mesh, for an interior vertex v_i, the discrete Gauss curvature

$$K_i = 2\pi - \sum_{f_{ijk} \in F} \alpha_i^{jk}, \quad (4)$$

where α_i^{jk} represents the corner angle attached to vertex v_i in the face f_{ijk}. Similarly, for a boundary vertex, the discrete Gauss curvature is

$$K_i = \pi - \sum_{f_{ijk} \in F} \alpha_i^{jk}. \quad (5)$$

Definition 6 (Discrete Ricci Flow) *An Euclidean triangle mesh with circle packing metric, the Euclidean Ricci flow is*

$$\frac{d\gamma_i(t)}{dt} = -K_i\gamma_i(t). \quad (6)$$

A Hyperbolic mesh with circle packing metric, the discrete Hyperbolic Ricci flow is

$$\frac{d\gamma_i(t)}{dt} = -K_i \sinh\gamma_i(t) \quad (7)$$

The following theoretic results guarantee the convergence of the discrete Ricci flow.

Theorem 7 (Convergence of Discrete Ricci Flow) *The discrete Ricci flows 6 and 7 are convergent to the uniformization metric and the convergence rate is exponential.*

More theoretic details can be found in [Chow and Luo 2003].

Discrete Ricci flows can be treated as the gradient flows of minimizing special energies.

Definition 8 (Discrete Ricci Energy) *Let* $u_i = log\gamma_i$ *in Euclidean case, and* $u_i = ln\tanh\frac{\gamma_i}{2}$*, then both the Euclidean Ricci energy and Hyperbolic Ricci energy are defined as*

$$f(\mathbf{u}) = \int_{\mathbf{u}_0}^{\mathbf{u}} \sum_{i=1}^{n} K_i du_i, \quad (8)$$

where $\mathbf{u} = (u_1, u_2, \cdots, u_n)$, $\mathbf{u}_0 = (0, 0, \cdots, 0)$.

4 ALGORITHMS TO COMPUTE GEODESIC SPECTRA OF SURFACES

This section introduces the algorithms for computing geodesic spectra in details for surfaces with different topologies.

4.1 Genus Zero Surfaces

All closed genus zero surfaces are conformally equivalent. That means they are indistinguishable under their conformal structures. For genus zero surfaces with boundaries, their conformal structures are not identical any more. For example, for genus zero surfaces with three boundaries, there are infinite conformally equivalent classes, which form a 3 dimensional space.

Figure 1 gives an example for genus zero surfaces with three boundaries.

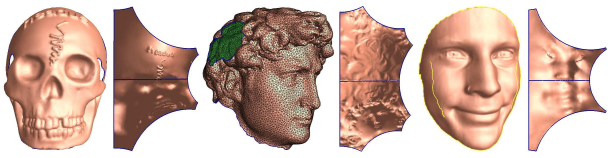

Figure 1: Conformal structures of the genus zero surface with 3 boundaries are determined by the lengths of the boundaries under the uniformization metric.

4.2 Genus One Surfaces

By the Uniformization theorem, a surface Σ with zero Euler number can be represented as $\mathbb{R}^2/Deck(\Sigma)$, where the deck transformation group consists of translations mapping the Euclidean plane $\mathbb{R}^2$ onto itself. The set of the lengths of closed geodesics on Σ can be computed algebraically from group $Deck(\Sigma)$. Therefore the whole procedure is to compute Euclidean Uniformization metric first, then the deck transformation group generators and finally the geodesic spectrum.

4.2.1 Computing Euclidean Uniformization Metric

The flat uniformization metric on a genus one closed surface can be induced either by the holomorphic 1-forms on it or discrete Euclidean Ricci flow. The algorithms for computing holomorphic 1-forms are introduced in [Gu and Yau 2003a] and [Jin et al. 2004]. Here we introduce the algorithm for computing the Euclidean uniformization metric using discrete Euclidean Ricci flow.

Given a triangular mesh, we first compute a circle packing metric $\{\Gamma,\Phi\}$ to approximate its induced Euclidean metric. Then we use Newton's method to minimize the Euclidean Ricci energy 8. The Hessian matrix of the energy is

$$\frac{\partial^2 f}{\partial u_i \partial u_j} = \frac{\partial K_i}{\partial u_j} = \frac{\partial K_i}{\partial \gamma_j}\gamma_j,$$

The Hessian matrix can be easily verified to be positive definite, therefore the energy is strictly convex, with a unique global minimum. Newton's method can be used to find the minimum with stable convergence.

4.2.2 Computing Deck Transformation Group Generators in the Plane

Computing Canonical Fundamental Group Generators
We first compute a set of canonical fundamental group generators $\{a_1,b_1\}$. From definition, a_1 and b_1 are closed loops and with only one geometric intersection point. The algorithms to compute the canonical fundamental group generators have been studied in computational topology and computer graphics literature. We adopted the methods introduced in [Carner et al. 2005] directly because of its simplicity.

The surface Σ is then sliced open along the fundamental group generators to form a topological disk D, which is a canonical fundamental domain, with its boundary taking the form $\partial D = a_1 b_1 a_1^{-1} b_1^{-1}$.

Embedding in the Plane
Let $\rho : D \to \mathbb{R}^2$ denote the desired isometric embedding of D under the uniformization flat metric. We randomly choose f_{012} in D as a seed face, and simply set the parametric position of v_0, v_1, and v_2, as follows: $\tau(v_0) = (0,0)$, $\tau(v_1) = (l_{01},0)$, $\tau(v_2) = l_{02}(\cos\theta_0, \sin\theta_0)$. Then we put faces sharing one edge with the seed face into a queue.

We pop a face f_{ijk} out of the queue. If all vertices have been embedded, we continue to pop another face out of the queue. Otherwise, assume v_k has not been embedded, v_i and v_j have embedded already. Then the parametric position $\rho(v_k)$ is the intersection of two circles $(\rho(v_i), l_{ik})$ and $(\rho(v_j), l_{jk})$. Also, the orientation of $\rho(v_i), \rho(v_j), \rho(v_k)$ should be counter clock wise. Then, we put all faces sharing one edge with f_{ijk} into the queue. We repeat embedding faces out of the queue until the queue is empty.

Figure 2 shows the genus one closed kitten model marked with a set of canonical fundamental group generators and its embedding in plane with Euclidean uniformization metric.

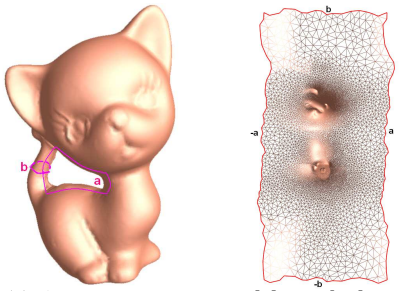

Figure 2: (a) Genus one Kitten model, marked with a set of canonical fundamental group generators $\{a,b\}$. (b) Embedded in the plane $\mathbb{R}^2$ with Euclidean Uniformization metric.

Computing Deck Transformation Group Generators
Deck transformations of a genus one closed surface are simply translations in the plane.

The image of the embedding of D has four different sides, $\rho(a), \rho(b), \rho(a^{-1}), \rho(b^{-1})$ (see Fig 2(b)). a coincides with a^{-1} in original kitten model, same as b and b^{-1}.

A deck transformation $\beta : \mathbb{R}^2 \to \mathbb{R}^2$ maps $\rho(a^{-1})$ to $\rho(a)$, therefore the boundary segment $\rho(a)$ of $\rho(D)$ coincides the boundary segment $\rho(a^{-1})$ of $\beta \circ \rho(D)$, two fundamental domains $\rho(D)$ and $\beta \circ \rho(D)$ are glued along the common boundary segment as shown in figure 3 (a). Suppose p is an interior point on the mesh, we choose an arbitrary path $\overline{\gamma}$ connecting $\rho(p)$ and $\beta \circ \rho(p)$ either the blue curve or the green curve in 3 (a), the projection of $\gamma = \pi(\overline{\gamma})$ is a closed loop on Σ, which is homotopic to b, therefore the deck transformation β corresponds to the homotopy class b, $\Phi(\beta) = b$. We can choose γ as the straight line segment, then γ is one geodesic homotopic to b.

Similarly, we can find another deck transformation α, such that $\alpha \circ \rho(b) = \rho(b^{-1})$, then α corresponds to a.

The two translations $\{\alpha,\beta\}$ are the generators of $Deck(\Sigma)$ for the kitten model. We can periodically embed D onto $\mathbb{R}^2$ with elements of group $Deck(\Sigma)$ and compute the closed geodesics for each homotopy class as illustrated in Figure 6(a).

4.2.3 Computing Geodesic Spectrum

All elements in the fundamental group of Σ has the form $\gamma_{m,n} = ma + nb$, therefore the corresponding deck transformation is $\tau_{m,n} = \alpha^m \circ \beta^n$. All deck transformations are translations. We use a planar vector to represent each deck transformation. In practice, we normalize α to be $(1,0)$ by scaling and rotating on $\mathbb{R}^2$, this won't affect the conformal structure of Σ, assume $\beta = (x,y)$, then $\tau_{m,n} = (m+nx, ny)$, the geodesic length in homotopy class $\gamma_{m,n}$ is $\sqrt{(m+nx)^2 + n^2y^2}$. Figure 6 shows a finite portion of the universal covering space embedded in the plane with the pre-images of geodesics,straight line segments.

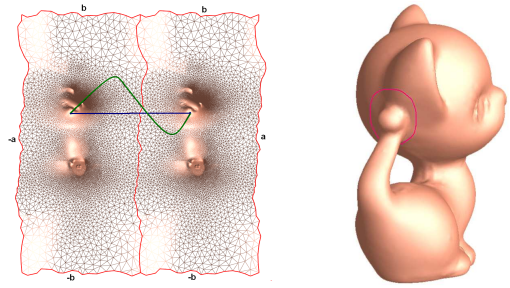

Figure 3: (a) One deck transformation which maps the left period to the right one, which corresponds to b^{-1}. (b) Two closed loops homotopic to the pink one on the kitten model lift as blue and green paths.

4.3 High Genus Surfaces

The computation for geodesic spectra of closed surfaces Σ with negative Euler number is very similar but more complicated. The whole procedure to compute Geodesic Spectra for a given surface with negative Euler number is as follows:
1. Computing hyperbolic uniformization metric of the surface Σ.
2. Computing its Fuchsian group generators in the hyperbolic space using Poincaré model.
3. Converting the deck group generators to the matrix representations in the upper half plane model, then computing the multipliers of deck transformations, which give the geodesic spectrum.

4.4 Computing hyperbolic uniformization metric

Similarly as computing Euclidean uniformization metric using Discrete Euclidean Ricci flow, we compute the Hyperbolic uniformization metric using Discrete Hyperbolic Ricci flow. First, we compute a circle packing metric on Σ to approximate the induced Euclidean metric on Σ. Then we minimize the hyperbolic Ricci energy 8 using Newton's method, for more details in [Jin et al. 2006].

4.5 Computing Fuchsian Group Generators in the Poincaré Disk Model

Computing Fundamental Group Generators
This step is exactly the same as for genus one closed surfaces. We use the same method [Carner et al. 2005] to compute a set of canonical fundamental group generators $\{a_1, b_1, a_2, b_2, \cdots, a_g, b_g\}$ for surface with genus g larger than one, then slice the surface open along the fundamental group generators to form a topological disk D. The boundary of D has the form $\partial D = a_1 b_1 a_1^{-1} b_1^{-1} a_2 b_2 a_2^{-1} b_2^{-1} \cdots a_g b_g a_g^{-1} b_g^{-1}$.

Isometric Embedding in Hyperbolic Disk
Then we isometrically embed D onto the Poincaré disk using the Hyperbolic uniformization metric computed from the first step, details in [Jin et al. 2006].

Figure 4 shows the original vase model and its embedding in the Poincaré disk with the Hyperbolic Uniformization metric.

Fuchsian Group Generators
Given two pairs of points p_0, q_0 and p_1, q_1 in the Poincaré

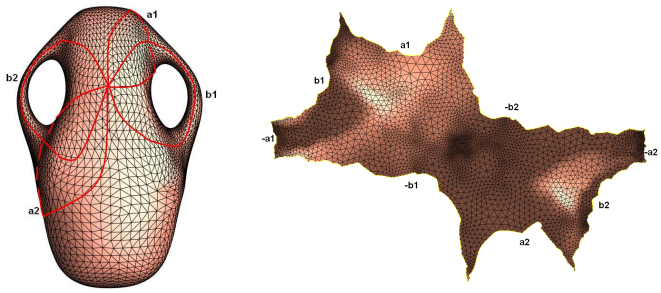

Figure 4: (a) Vase model marked with a set of canonical fundamental group generators. (b) Embedded in the Poincaré disk with the Hyperbolic Uniformization metric

disk, such that the geodesic distance from p_0 to q_0 equals to the geodesic distance from p_1 to q_1. Then there is a unique Möbius transformation τ, such that $p_1 = \tau(p_0)$ and $q_1 = \tau(q_0)$. τ can be constructed in the following way: Construct a Möbius transformation τ_0 to map p_0 to the origin, q_0 to a positive real number, with

$$\tau_0 = e^{-i\theta_0} \frac{z - p_0}{1 - \bar{p_0} z}, \theta_0 = arg \frac{q_0 - p_0}{1 - \bar{p_0} q_0}.$$

Similarly, we can define a Möbius transformation τ_1, which maps p_1 to the origin, q_1 to a real number, and $\tau_1(q_1)$ must equals to $\tau_0(q_0)$. Then the desired Möbius transformation τ is $\tau = \tau_1^{-1} \circ \tau_0$. Generators for Fuchsian group are Möbius transformations and can be constructed in a similarly way.

Let $\{\rho(a_k), \rho(a_k^{-1})\} \subset \partial D$ are two boundary curve segments. We want to find a Möbius transformation β_k, such that $\beta_k(\rho(a_k^{-1})) = \rho(a_k)$. Let their starting and ending vertices are $\partial\rho(a_k^{-1}) = \{q_0, p_0\}$ and $\partial\rho(a_k) = \{p_1, q_1\}$, then the Möbius transformation β_k maps (p_0, q_0) to (p_1, q_1). β_k is the Fuchsian generator corresponding to b_k. Similarly, we can compute α_k which maps $\rho(b_k)$ to $\rho(b_k^{-1})$. Therefore, we can compute a set of canonical Fuchsian group generators $\{\alpha_1, \beta_1, \alpha_2, \beta_2, \cdots, \alpha_g, \beta_g\}$.

Figure 5(a) shows one Fuchsian group generator acting on the fundamental domain of a vase model. The two red points are the pre-images of a same point on the vase model. Paths connecting them are projected to closed loops homotopic to the red curve on vase model, see Figure 5(b). Figure 6(b) shows a finite portion of the universal covering space of vase model embedded in the Poincaré disk model, generated by the actions of Fuchsian group elements.

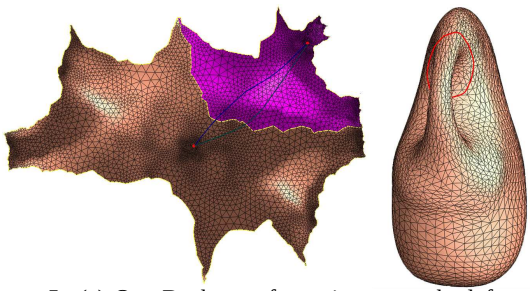

Figure 5: (a) One Deck transformation maps the left period to the right one. (b) Two closed loops homotopic to the red one on the vase model lift as two blue Paths in the universal covering space.

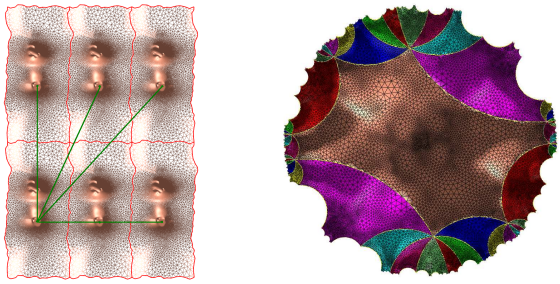

Figure 6: (a) A finite portion of the universal covering space of kitten model, generated by the actions of deck transformation group elements. (b) A finite portion of the universal covering space of vase model, generated by the actions of Fuchsian group elements.

4.6 Computing Geodesic Spectra of Surface

After computing the Fuchsian group generators, the geodesic spectrum of the surface can be algebraically computed in a straightforward way. Suppose Σ is a closed surface (if Σ is open, we use its double covering) with hyperbolic uniformization metric, $\{a_1, b_1, a_2, b_2, \cdots, a_g, b_g\}$ is a set of fundamental group generators and $\{\alpha_1, \beta_1, \alpha_2, \beta_2, \cdots, \alpha_g, \beta_g\}$ is the set of corresponding Fuchsian group generators. we want to compute the length of the geodesic in the homotopy class $\gamma = w_1 w_2 \cdots w_n$, where w_k is one of the a_i's or b_i's. We replace a_i in γ by α_i, b_j by β_j in γ to get a Fuchsian transformation τ. For example, Suppose $\gamma = a_1 b_1 a_1^{-1} b_1^{-1}$, then its corresponding Fuchsian transformation is $\tau = \alpha_1 \beta_1 \alpha_1^{-1} \beta_1^{-1}$. We transform τ from Poincaré disk model to upper half plane model with $h^{-1} \circ \tau \circ h$ using formulae 1.

Denoting the length of the geodesic homotopy to γ as l, with the trace of the matrix τ satisfying the following relation: $tr(h^{-1} \circ \tau \circ h) = 2\cosh(\frac{l}{2})$, the geodesic length l can be derived as:

$$l = 2acosh(\frac{tr(h^{-1} \circ \tau \circ h)}{2}) \tag{9}$$

5 EXPERIMENTAL RESULTS

The algorithm introduced in above sections for computing geodesic spectrum from Möbius transformations is purely algebraic, easy to implement and fast to compute. In this section, in order to verify our algorithm, we performed extensive experiments on general triangular meshes with complicated topologies.

Figure 7(a) shows six genus one closed surfaces. Table 1 lists part of their geodesic spectra, lengths of the first 8 shortest geodesic. And figure 8(a) depicts the spectra for easier comparison purpose.

Figure 8(b) and Table 2 demonstrate the experimental results for genus three surfaces in Figure 7.

Because the geodesic spectrum indicates the conformal structures, the experimental results show that all the surfaces are conformally inequivalent.

The programs are coded in C++ and on Windows platform. The most time consuming part of the pipeline is the computation of uniformization metric. Due to page limit, we refer readers to [Jin et al. 2006] for time table of computing uniformization metric. The experimental results shows the algorithm is efficient and robust.

model	Geodesic Spectra of Genus One Surfaces			
Kitten	1.00000	2.00000	2.17160	2.38896
	2.39265	2.94930	2.95526	2.99999
Teapot	1.00000	2.00000	3.00000	3.02754
	3.18818	3.18865	3.62808	3.62893
Rocker Arm	1.00000	1.29513	1.62606	1.64638
	2.00001	2.36872	2.39663	2.59026
Torus	1.00000	2.00000	2.29208	2.50072
	2.50072	3.00000	3.04198	3.04198
Elk	1.00000	2.00000	3.00000	3.76495
	3.89411	3.89687	4.26068	4.26570
Knot	1.00000	1.99999	2.99999	3.99999
	4.99999	5.99999	6.99999	7.99999

Table 1: Geodesic Spectrum of Genus One Surfaces.

model	Geodesic Spectra of Genus Three Surfaces			
David	0.837531	1.031991	1.092184	1.675063
	2.063981	2.184367	3.369938	3.549802
	3.728019	4.276527	4.402193	4.499322
Genus3	2.608251	2.750676	2.848831	3.841951
	3.841954	3.841958	3.841965	5.032769
	5.216501	5.225431	5.290124	5.423762
Three-Hole	1.676075	1.690413	1.708316	3.319118
	3.352150	3.380825	3.393546	3.409811
	3.416633	3.977163	4.040855	4.054275
Holes3	2.349592	2.354404	2.358875	2.376324
	2.702315	3.588764	3.605088	3.614748
	3.675990	3.698398	4.699184	4.708807

Table 2: Geodesic Spectrum of Genus Three Surfaces.

6 Conclusion

In this paper, we introduce a rigorous and efficient algorithm to compute the geodesic spectrum for surfaces with non-positive Euler number with uniformization metrics, which indicates the conformal structure of the surface. The method can be applied for surface classification, shape comparison and shape retrieval purposes.

Geodesic spectra are not only for conformal structures, they are also reflect the information of the Riemannian metrics. It is still an open problem for computing closed geodesics for general surfaces embedded in $\mathbb{R}^3$. In the future, we will explore

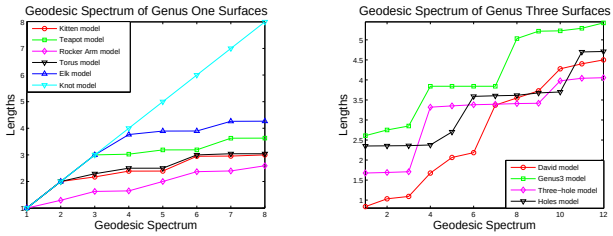

Figure 8: (a) Comparison of geodesic spectrum of genus one models. (b) Comparison of geodesic spectrum of genus three models.

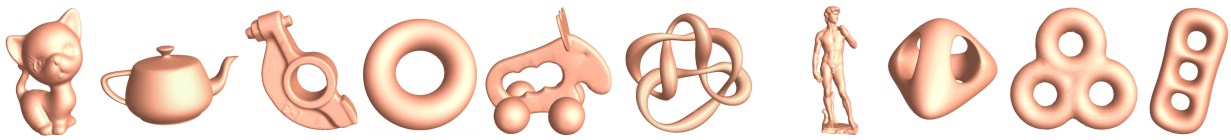

Figure 7: From left to right, genus one models: Kitten model, Teapot model, Rocker Arm model, Torus model, Elk model, Knotty torus Model; genus three models: David model, Genus3 model, Three-Hole model, Holes3 model.

along this direction to find geodesic spectra for general Riemannian manifolds. The discrete Ricci flow and hyperbolic geometry method can be applied for much broader applications such as surface parametrization and shape matching, registration, spline construction. In the future, we will investigate further on these related applications.

References

BOBENKO, A., AND SCHRODER, P. 2005. Discrete willmore flow. In *Eurographics Symposium on Geometry Processing*.

CARNER, C., JIN, M., GU, X., AND QIN, H. 2005. Topology-driven surface mappings with robust feature alignment. In *IEEE Visualization*, 543–550.

CHEN, J., AND HAN, Y., 1996. Shortest paths on a polyhedron; part i: computing shortest paths.

CHOW, B., AND LUO, F. 2003. Combinatorial ricci flows on surfaces. *Journal Differential Geometry 63*, 1, 97–129.

DEY, T. K. 1994. A new technique to compute polygonal schema for 2-manifolds with application to null-homotopy detection. In *SCG '94: Proceedings of the tenth annual symposium on Computational geometry*, ACM Press, New York, NY, USA, 277–284.

ELAD, A., AND KIMMEL, R., 2003. On bending invariant signatures for surfaces.

ÉRIC COLIN DE VERDIÉRE, AND LAZARUS, F. 2002. Optimal system of loops on an orientable surface. In *FOCS '02: Proceedings of the 43rd Symposium on Foundations of Computer Science*, IEEE Computer Society, Washington, DC, USA, 627–636.

GU, X., AND YAU, S.-T. 2003. Global conformal parameterization. In *Symposium on Geometry Processing*, 127–137.

GU, X., AND YAU, S.-T. 2003. Surface classification using conformal structures. In *International Conference on Computer Vision*.

GU, X., HE, Y., AND QIN, H. 2005. Manifold splines. In *Symposium on Solid and Physical Modeling*, 27–38.

HAMILTON, R. S. 1988. The ricci flow on surfaces. *Mathematics and general relativity 71*, 237–262.

HETROY, F. 2005. Constriction computation using surface curvature. In *Eurographics (short papers)*, J. Dingliana and F. Ganovelli, Eds., Eurographics, 1–4.

HILAGA, M., SHINAGAWA, Y., KOHMURA, T., AND KUNII, T. L. 2001. Topology matching for fully automatic similarity estimation of 3d shapes. In *SIGGRAPH '01: Proceedings of the 28th annual conference on Computer graphics and interactive techniques*, ACM Press, New York, NY, USA, 203–212.

JIN, M., WANG, Y., YAU, S.-T., AND GU, X. 2004. Optimal global conformal surface parameterization. In *IEEE Visualization*, 267–274.

JIN, M., LUO, F., AND GU, X. 2006. Computing surface hyperbolic structure and real projective structure. In *SPM '06: Proceedings of the 2006 ACM symposium on Solid and physical modeling*, ACM Press, New York, NY, USA, 105–116.

KANEVA, B., AND OROURKE, J. 2000. An implementation of chen and hans shortest paths algorithm. In *Proc. of the 12th Canadian Conf. on Comput. Geom.*, 139C146.

KAPOOR, S. 1999. Efficient computation of geodesic shortest paths. In *STOC '99: Proceedings of the thirty-first annual ACM symposium on Theory of computing*, 770–779.

KHAREVYCH, L., SPRINGBORN, B., AND SCHRODER, P. 2005. Discrete conformal mappings via circle patterns.

KIMMEL, R., AND SETHIAN, J. A. 1998. Computing geodesic paths on manifolds. *Proc. of National Academy of Sci. 95*, 15, 8431C8435.

MIKA SEPPALA, T. S. 1992. *Geometry of Riemann surfaces and Teichmuller spaces*. North-Holland Math Stud.

MITCHELL, J. S. B., MOUNT, D. M., AND PAPADIMITRIOU, C. H. 1987. The discrete geodesic problem. *SIAM J. Comput. 16*, 4, 647–668.

OSADA, R., FUNKHOUSER, T., CHAZELLE, B., AND DOBKIN, D. 2001. Matching 3d models with shape distributions. In *Shape Modeling International*, 154–166.

REUTER, M., WOLTER, F.-E., AND PEINECKE, N. 2005. Laplace-spectra as fingerprints for shape matching. In *SPM '05: Proceedings of the 2005 ACM symposium on Solid and physical modeling*, ACM Press, New York, NY, USA, 101–106.

STEPHENSON, K. 2005. *Introduction To Circle Packing*. Cambridge University Press.

SURAZHSKY, V., SURAZHSKY, T., KIRSANOV, D., GORTLER, S. J., AND HOPPE, H. 2005. Fast exact and approximate geodesics on meshes. *ACM Trans. Graph. 24*, 3, 553–560.

THURSTON, W. 1976. *Geometry and Topology of 3-manifolds*. Princeton lecture notes.

THURSTON, W. P. 1997. *Three-Dimensional Geometry and Topology*. Princeton University Presss.